Carcinogenesis vol.31 no.11 pp.1922–1931, 2010
doi:10.1093/carcin/bgq170
Advance Access publication August 12, 2010

Unexpected role for the human Cx37 C1019T polymorphism in tumour cell proliferation

Sandrine Morel[1,2,*], Laurent Burnier[1,2], Angela Roatti[1,2], Alexandra Chassot[1,2], Isabelle Roth[2], Esther Sutter[1,2], Katia Galan[1,2], Anna Pfenniger[1,2], Marc Chanson[3] and Brenda R.Kwak[1,2]

[1]Department of Pathology and Immunology, [2]Division of Cardiology, Department of Internal Medicine and [3]Department of Pediatrics, University of Geneva and Geneva University Hospitals, CH-1211 Geneva, Switzerland

[*]To whom correspondence should be addressed. Fondation Recherche Medicale, Cardiology, University of Geneva, 64 avenue de la Roseraie, CH-1211 Geneva, Switzerland. Tel: + 41 22 382 72 36;
Fax: +41 22 382 72 45;
Email: sandrine.morel@unige.ch

Connexins are a large family of proteins that form gap junction channels allowing exchange of ions and small metabolites between neighboring cells. They have been implicated in pathological processes such as tumourigenesis in which they may act as tumour suppressors. A polymorphism in the human connexin37 (Cx37) gene (C1019T), resulting in a non-conservative amino acid change in the regulatory C-terminus (CT) of the Cx37 protein (P319S) has been suggested to be implicated in predisposition to angiosarcomas. In this study, we have used communication-deficient HeLa and SK-HEP-1 cells transfected with Cx37-319S, Cx37-319P or empty vector. We showed that the expression of Cx37-319P limited proliferation of HeLa and SK-HEP-1 cells, whereas Cx37-319S expression was without effect. Using an *in vitro* kinase assay, we demonstrated phosphorylation of Cx37 CT by glycogen synthase kinase-3 (GSK-3), a kinase known to be implicated in cell proliferation and cancer. GSK-3-induced phosphorylation was associated with reduced gap junctional intercellular communication (GJIC) as measured by microinjection of the tracer neurobiotin. Inhibition of GSK-3 by LiCl or SB415286 reduced phosphorylation of Cx37-319P and increased GJIC. This latter effect on GJIC involved the beta and not the alpha isoform of GSK-3. In contrast, GSK-3 inhibitors were without effect on HeLa cells expressing Cx37-319S. In conclusion, our data indicate functional effects of the Cx37 C1019T polymorphism on GJIC that might contribute to tumour cell growth.

Introduction

Gap junctional intercellular communication (GJIC) is essential to maintain tissue homeostasis by transferring second messengers and small metabolites between adjacent cells (1–3). Gap junction channels are oligomeric assemblies of connexins (Cx), members of a large family of related proteins. Six connexins assemble into a hemichannel or connexon, and a complete gap junction channel is formed by the docking with a hemichannel of the neighboring cell. Functional replacement of one connexin gene with another revealed that cellular homeostasis depends on types of connexin expressed (4). This implies that the specific trafficking, permeability as well as interaction with transduction networks of each connexin type is contributing to tissue response (5).

GJIC is impaired in cancer tissues, which is generally considered to contribute to aberrant growth of tumour cells (6,7). The lack of GJIC among cancer cells may be the consequence of two separate phenomena, i.e. a lack of expression or an aberrant localization of the connexins (8–10). Interestingly, transfection of connexin genes in GJIC-deficient tumour cells restores normal cell growth *in vitro* and *in vivo* (6,11–15). These tumour-suppressive actions of connexin genes seem, however, specific for the type of connexins and cells studied (6,7).

Because many tumour suppressor genes are mutated in cancer, the occurrence of connexin gene mutations has been studied in various types of tumours (16). Several studies have focused on Cx37 after an initial report identifying tumour-associated antigenic peptides from two mouse Lewis lung carcinoma cell lines (3LL and CMT) that showed a strong sequence homology to (mutated) Cx37 protein (17). Although DNA from these cell lines did not harbour the proposed Cx37 mutations (18), other mutations were detected in this gene in hepatic angiosarcomas from rats treated with vinyl chloride (19). Moreover, immunohistochemical analysis in these angiosarcomas failed to detect Cx37 at cell-to-cell contacts, whereas it was readily observable in endothelial cells of normal liver.

A polymorphism in the human Cx37 gene (C1019T), resulting in a non-conservative amino acid change (P319S) in the regulatory C-terminus (CT) of the Cx37 protein, has been proposed as prognostic marker for coronary artery disease and myocardial infarction (see refs. for reviews 20,21). Using atherosclerosis-susceptible mice and transfected mononuclear cells, we have previously demonstrated that polymorphic Cx37 channels may function as prognostic markers for atherosclerosis (22,23). The Cx37 C1019T polymorphism has also been investigated in patients with hepatic angiosarcomas (24). These rare malignant neoplasms arise from vascular endothelial cells and have been linked to exposure to chemicals such as vinyl chloride or Thorotrast (25,26). Although the authors suggested a tendency towards over-representation of the *1019T* allele, coding for Cx37-319S, in patients with vinyl chloride-induced tumours, this observation remained inconclusive due to the very small sample number.

In the present study, we have compared cell proliferation between communication-deficient cells (HeLa and SK-HEP-1) and cells stably expressing similar levels of Cx37-319S and Cx37-319P. Our results show decreased proliferation of cells expressing Cx37-319P. This reduced proliferation is not due to differences in cell adhesion or cell death between the clones. Moreover, we have identified a unique site in Cx37-319P for phosphorylation by glycogen synthase kinase 3 (GSK-3), a Ser/Thr kinase that is implicated in multiple cellular processes and pathologies, including cell proliferation and cancer (reviewed in refs. 27,28). Finally, we show that inhibition of GSK-3β equilibrates GJIC between Cx37-319S- and Cx37-319P-expressing HeLa cells. Overall, our data indicate functional effects of the Cx37 C1019T polymorphism on GJIC that might contribute to tumour cell growth.

Abbreviations: ATP, adenosine triphosphate; CT, C-terminus; DMSO, dimethyl sulfoxide; EV, empty vector; FBS, fetal bovine serum; GJIC, gap junctional intercellular communication; GSK-3, glycogen synthase kinase-3; NS, not significant; SDS, sodium dodecyl sulphate; SiRNA, small interfering RNA.

Materials and methods

Cell cultures

Human HeLa cells (#CCL-2; American Type Culture Collection, Manassas, UA) and human SK-HEP-1 cells (#HTB-52; American Type Culture Collection) were transfected with plasmids coding for human Cx37 polymorphisms as described previously (23). The transfected human cell lines expressing Cx37-319P, Cx37-319S or empty vector (EV) pIRES2-eGFP were grown in Dulbecco's modified Eagle's medium supplemented with 10% fetal bovine serum (FBS), 50 U/ml penicillin and 50 μg/ml streptomycin (Gibco BRL, Basel, Switzerland). Transfected cells were under continuous selection pressure with 300 μg/ml G418 (Gibco BRL) for HeLa cells and 500 μg/ml G418 for SK-HEP-1 cells.

Cell proliferation assay

Cell proliferation was evaluated by two methods: one determining the number of adherent cells only and another accounting for adherent and non-adherent cells. For the first method, 5000 HeLa cells from each clone were inoculated in

triplicate into 96-well microtiter plate and kept in regular medium at 37°C to permit their adhesion. When adhesion was complete, medium was removed and HeLa cells were maintained overnight in culture in medium without FBS (Dulbecco's modified Eagle's medium supplemented with 5% bovine serum albumin). To evaluate proliferation, HeLa cells were cultured for 48 h in regular medium with FBS. At the end of this 2 day period, cells were stained for 10 min with 0.1% crystal violet in 20% methanol (prepared in water) after which the unbound dye was removed in tap water and the plate was air-dried (29). The bound dye was solubilized in 2% sodium dodecyl sulphate (SDS) and the absorbance of the samples was measured at 570 nm with a spectrophotometer. Cell number was calculated using calibration curves made for each clone.

For the second method, 5000 HeLa cells and 10 000 SK-HEP-1 cells of each clone were grown as described above. At the end of the 2 day period, cell proliferation was evaluated by using 'CellTiter 96 Aqueous One Solution Cell Proliferation Assay' (Promega AG, Dubendorf, Switzerland). For this assay, solution containing tetrazolium compound was added in each well for 90 min at 37°C. Viable cells (adherent and non-adherent cells) reduced the tetrazolium compound and absorbance was read at 490 nm (T48). Results obtained from HeLa and SK-HEP-1 cells transfected with Cx37-319P were expressed in fold increase of cells transfected with Cx37-319S. To verify that initial number of cells was similar between the two clones after overnight culture in medium without FBS (T0), quantification of adherent cells was performed by replacing culture medium by fresh medium and then adding tetrazolium compound. Proliferation of HeLa cells was also quantified in presence of 50 U/ml apyrase or 200 μM adenosine triphosphate (ATP) (Sigma–Aldrich, Buchs, Switzerland) (22). In addition, HeLa and SK-HEP-1 transfectants were cultured in parallel dishes to verify equal Cx37 expression.

Cell death analysis

Death of HeLa cells after 2 days in culture was analysed by different methods. First, the number of dead cells in culture dish supernatant was determined with Trypan blue. Secondly, uncleaved and cleaved caspase-3 expression was evaluated by western blot. Finally, cell death was analysed by Fluorescence Activated Cell Sorting. For this purpose, HeLa cells were incubated with phycoerythrin Annexin V and 7-aminoactinomycin D for 30 min in the dark (PE Annexin V Apoptosis Detection Kit I; BD Biosciences, Allschwill, Switzerland).

Protein extraction and western blotting

Proteins were extracted from transfected HeLa or SK-HEP-1 cells in modified RIPA buffer as described previously (23). Western blotting was performed using antibodies against Cx37 (Alpha Diagnostics, VWR, Dietikon, Switzerland), uncleaved and cleaved Caspase-3 (Cell Signaling Technology, Allschwill, Switzerland), phospho-GSK-3β (Ser9) (Cell Signaling Technology, Allschwill, Switzerland), total-GSK-3β (Cell Signaling Technology, Allschwill, Switzerland), phospho-GSK-3α (Ser21) (Cell Signaling Technology, Allschwill, Switzerland), total-GSK-3α (Cell Signaling Technology, Allschwill, Switzerland), phospho-β-catenin (Ser33/Ser37/Thr41) (Cell Signaling Technology, Allschwill, Switzerland), total-β-catenin (Cell Signaling) and Glyceraldehyde 3-phosphate dehydrogenase (Chemicon, Basel, Switzerland).

Prediction of phosphorylation sites and associated kinases in Cx37-319S and Cx37-319P

The prediction of phosphorylated amino acids was performed with the NetPhos 2.0 Server and of the kinases involved with the NetPhosK 1.0 server (30). Prediction analysis was done with evolutionary stable sites and with a threshold of 0.5.

Production and purification of recombinant CT of Cx37-319S and Cx37-319P

Production of the CT tail of Cx37-319S and Cx37-319P (Cx37CT-319S and Cx37CT-319P) was performed using methods described previously (31,32). Cx37CT-319P was produced in BL-21 competent cells by introducing human complementary DNA into pGEX-6P-2 plasmids (Amersham, Glattbrugg, Switzerland). The resultant Glutathion-S-transferase-fusion protein was cleaved to obtain amino acids 233–333 of human Cx37 (Cx37CT-319P). The Cx37CT-319S clone was produced using the QuickChange Site-Directed Mutagenesis Kit (Stratagene, Santa Clara, CA) on the Cx37CT-319P pGEX-6P-2 plasmid. The following primers were used: forward, GAATGGCCAAAAATCCCCAAGTCGTC and reverse, GACGACTTGGGGATTTTTGGCCATTC. For the two Cx37CT peptides, protein concentration was measured with the Bio-Rad DC Protein Assay and purity was assessed by SDS–polyacrylamide gel electrophoresis and Coomassie staining.

In vitro kinase assay

Phosphorylation of the CT tail of Cx37-319S and Cx37-319P by GSK-3β was tested by an *in vitro* kinase assay in the presence of an active recombinant GSK-3β. Cx37CT-319S and Cx37CT-319P were incubated with 1 μg of active recombinant GSK-3β (Biovision, Mountain View, CA) for 30 min at 30°C in kinase buffer [25 mM Tris–HCl (pH 7.5), 5 mM β-glycerophosphate, 12 mM $MgCl_2$, 2 mM dithiothreitol, 1 mM sodium orthovanadate and a cocktail of proteases inhibitors (Roche, Basel, Switzerland)] supplemented with 200 μM ATP (Sigma–Aldrich) and 10 μCi [γ-^{32}P]ATP. The reaction was stopped by adding SDS buffer. Samples were heated at 95°C for 10 min, followed by electrophoresis on a 15% polyacrylamide gel. The gels were stained with Coomassie blue, dried and exposed overnight on a hyperfilm MP (Amersham). Signals were quantified using NIH AutoExtractor 1.51 software.

The kinase assays were performed in presence of vehicle [H_2O or dimethyl sulfoxide (DMSO)] or GSK-3 inhibitors [10 mM LiCl and 50 μM SB415286 (Sigma–Aldrich)]. Optimal doses of GSK-3 inhibitors were determined in HeLa cells using different concentrations of LiCl (0–40 mM) and SB415286 (0–100 μM). The efficacy of inhibition of GSK-3 activity was evaluated by western blot by using antibodies against phospho-GSK-3β, total-GSK-3β, phospho-GSK-3α and total-GSK-3α for LiCl treatment and with antibodies against phospho-β-catenin and total-β-catenin for SB415286 treatment.

Immunofluorescence

Transfected HeLa cells were grown to confluence onto coverslips and fixed 10 min in methanol at −20°C. Cells were immunolabelled with Cx37 antibody (Alpha Diagnostics) as described previously (32). Cells were counterstained with Evans blue and nuclei were stained with 4′,6-diamidino-2-phenylindole. Staining was examined with a LSM 510 Meta confocal microscope (Carl Zeiss AG, Feldbacht, Switzerland) connected to a personal computer, and images were captured with the software provided by the manufacturer.

siRNA transfection

HeLa cells were transfected with 25 or 50 nM control small interfering RNA (siRNA) (Control Smart Pool 1; Thermo Scientific Dharmacon, [Lafayette, CO] or #1108188; Microsynth, Balgach, Switzerland), 25 nM siRNA-GSK-3α (# s6236; Thermo Scientific Dharmacon) or 50 nM siRNA-GSK-3β (#4390825; Applied Biosystem-Ambion, Rotkreuz, Switzerland) by using Lipofectamine RNAiMAX (Invitrogen, Basel, Switzerland). For this purpose, cells were incubated for 48 or 60 h with siRNA. Optimal doses of each siRNA were determined in HeLa cells using different concentrations of siRNA, and the efficacy of the specific inhibition of GSK-3 isoform expression was evaluated by western blot by using antibodies against total GSK-3β and total-GSK-3α.

Dye coupling

For analysis of cell-to-cell coupling, one HeLa cell within a cluster was impaled with a thin tip microelectrode filled with 1% Lucifer yellow and 2% neurobiotin solution prepared in 150 mM KCl and buffered to pH 7.2 with 10 mM *N*-2-hydroxyethylpiperazine-*N*′-2-ethanesulfonic acid–KOH. The tracers were allowed to fill the cells by simple diffusion for 3 min (33). Lucifer yellow was added to the microelectrode solution to visualize and mark the injected cell. At the end of the injection, the electrode was removed and cells were fixed with 4% paraformaldehyde. After permeabilization with 0.3% Triton X-100, neurobiotin diffusion was revealed with streptavidine–rhodamine (1/3000) for 60 min at room temperature. Fluorescent cells were observed with an inverted TMD-300 microscope (Nikon, Egg, Switzerland) equipped with a ×40 phase 3 dark medium objective with a numerical aperture of 0.7 (Carl Zeiss). Images were captured with a Visicam digital camera (Visitron Systems, Puchheim, Germany) connected to a personal computer running Metafluor 4.01 software (Universal Imaging, Sunnyvale, CA). Numbers of stained cells were counted.

In a first set of experiments, parental HeLa cells and HeLa cells transfected with Cx37-319S or Cx37-319P were treated with vehicle (H_2O or DMSO) or GSK-3 inhibitors (10 mM LiCl or 50 μM SB415286) during 15 min before the microinjection. In a second set of experiments, HeLa cells were transfected with control siRNA, siRNA-GSK-3β or siRNA-GSK-3α during 48 or 60 h before the microinjections. Between 6 and 13 injections were performed for each condition.

Electrical coupling

For electrical coupling studies, the dual whole-cell patch clamp approach was applied on cell pairs. Patch electrodes were filled with (in mM) 139 KCl, 1 NaCl, 2 $MgCl_2$, 0.5 $CaCl_2$, 5.5 ethyleneglycol-bis(aminoethylether)-tetraacetic acid, buffered to pH 7.2 with 10 mM *N*-2-hydroxyethylpiperazine-*N*′-2-ethanesulfonic acid–KOH. The external solution was (in mM) 136 NaCl, 4 KCl, 1 $CaCl_2$, 1 $MgCl_2$, 10 *N*-2-hydroxyethylpiperazine-*N*′-2-ethanesulfonic acid and 2.5 glucose (pH 7.4). For some experiments, 10 mM LiCl was added to the bath solution 15 min before the recording. All experiments were carried out at room temperature.

Both cells of a pair were voltage-clamped at a common holding potential of 0 mV using an EPC-9 (HEKA Elektronik, Lambrecht, Germany) and a PC-501A amplifier (Warner Instruments, Hamden, CT). To measure gap junctional currents (I_j), transjunctional voltage steps (V_j) of 10 mV were applied. Gap junctional conductance (g_j) was then calculated by $g_j = I_j/V_j$. Series resistance was not compensated and was <2% of the combined junctional and cell input resistance.

Statistical analysis

The data are presented as mean ± SEM. Independent experiments were compared by Student's *t*-test. Differences indicated by an asterisk or a number sign were considered statistically significant at $P < 0.05$.

Results

Cx37 expression and cell proliferation in transfected HeLa and SK-HEP-1 cells

Clones of HeLa transfectants used in this study have been chosen for their equal expression level of total and membrane Cx37-319S and Cx37-319P, as described in detail elsewhere (23). To study the effect of polymorphic Cx37 on HeLa cell growth, cells were cultured during 48 h in 96-well plate. As shown in Figure 1A, Cx37 expression remained similar between HeLa Cx37-319S and Hela Cx37-319P transfectants, the first 2 days after passage during which the proliferation assays were performed. As shown in Figure 1B (left panel), cell growth in Cx37-319P-expressing HeLa cells was reduced compared with clones transfected with EV or with Cx37-319S ($P < 0.01$). Expression of Cx37-319S had no effect on HeLa cell growth. Using short-term (<30 min) adhesion assays, we have shown previously that mononuclear cells or HeLa cells transfected with Cx37-319P were less adhesive than cells expressing Cx37-319S due to an increased release of ATP (22,23). To verify that difference in proliferation between the two cell clones did not result from a difference in their initial adhesion, we performed another type of proliferation assay that takes non-adherent cells into account (Figure 1B, right panel). Whereas we started with an equal number of HeLa cells transfected with Cx37-319S or Cx37-319P after overnight incubation without FBS (T0), we confirmed that Cx37-319P-expressing cells exhibited reduced growth compared with Cx37-319S-expressing cells

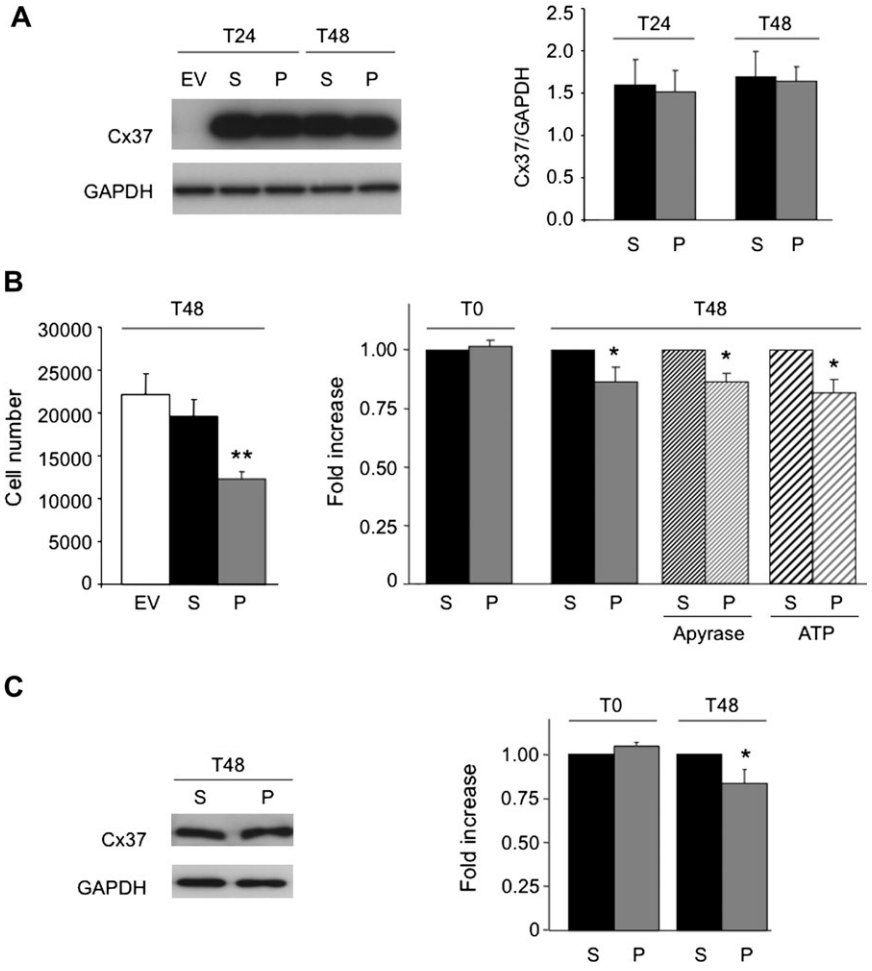

Fig. 1. Cx37 C1019T polymorphism and tumour cell proliferation. (**A**) Quantification of Cx37 by western blot showed that this protein is equally expressed in HeLa cells transfected with Cx37-319S and Cx37-319P 24 h (T24) and 48 h (T48) after cell passage. Figure shows representative western blots for Cx37 in HeLa cells transfected with EV, Cx37-319S (S) or Cx37-319P (P); $N = 7$. Glyceraldehyde 3-phosphate dehydrogenase (GAPDH) is used as loading control. (**B**) Left panel: cell number measured with crystal violet staining after 48 h in culture for the three HeLa cell transfectants (T48). Results are presented as mean of seven independent experiments, and each experiment was performed in triplicate. Right panel: cell proliferation measured by the reduction of tetrazolium compound in the culture medium before (T0) and after 48 h (T48) of proliferation. During the 48 h of proliferation, some cultures were treated with 50 U/ml apyrase or 200 μM ATP. Results are presented as mean of eight independent experiments, each experiment was performed in triplicate, and results obtained for HeLa Cx37-319P cells were expressed in fold increase of HeLa Cx37-319S cells. Error bars show SEM, $^{**}P < 0.01$ versus EV and Cx37-319S and $^{*}P < 0.05$ versus Cx37-319S. (**C**) Left panel: Cx37 western blot of SK-HEP-1 cells transfected with Cx37-319S or Cx37-319P. Glyceraldehyde 3-phosphate dehydrogenase (GAPDH) is used as loading control. Right panel: SK-HEP-1 cell proliferation measured by the reduction of tetrazolium compound in the culture medium before (T0) and after 48 h (T48) of proliferation. Results are presented as mean of six independent experiments, each experiment was performed in triplicate, and results obtained for SK-HEP-1 Cx37-319P cells were expressed in fold increase of SK-HEP-1 Cx37-319S cells. Error bars show SEM and $^{*}P < 0.05$ versus Cx37-319S.

after 48 h of proliferation (T48). Moreover, the differences in growth between Cx37-319S- and Cx37-319P-expressing cells were maintained in the presence of apyrase (an ATP scavenger) or ATP (22), further indicating that the observed differences in proliferation between the two clones were probably not caused by differences in cell adhesion. Finally, the growth-reducing effect of Cx37-319P was confirmed in SK-HEP-1 cells, a human endothelial cell line. Indeed, SK-HEP-1 transfectants expressing similar levels of Cx37-319P and Cx37-319S displayed a clear difference in proliferation after 48 h of culturing (T48), whereas the number of cells initially plated (T0) were equal (Figure 1C). Thus, difference in proliferation between the two cell clones is not caused by difference adhesion.

Next, we investigated whether the anti-proliferative effect of Cx37-319P was due to increased cell death, i.e. apoptosis or necrosis. As shown in the phase-contrast images in Figure 2A, HeLa cells transfected with Cx37-319S, Cx37-319P or EV were all able to grow to a confluent monolayer of cells. Counting the number of viable and dead cells present in the supernatant revealed no significant differences between the three clones. Thus, the number of viable cells (not stained with Trypan blue) in supernatant was 30 833 ± 6882, 37 500 ± 4743 and 37 917 ± 5568 [$N = 6$, not significant (ns)] for Hela EV, HeLa Cx37-319S and HeLa Cx37-319P, respectively. The number of dead cells (stained with Trypan blue) in supernatant was 25 000 ± 6090, 54 167 ± 14 034 and 52 500 ± 13 586 ($N = 6$, ns) for Hela EV, HeLa Cx37-319S and HeLa Cx37-319P, respectively. In addition, no cleaved Caspase-3 was observed in HeLa transfectants after 48 h of culture (Figure 2B). In contrast, when these HeLa cells were treated with 1 μM staurosporine to induce apoptosis, a 17 kDa band appeared indicative for cleaved Caspase-3 (Figure 2B). Finally, flow cytometry analysis showed that total cell death was similar between the three clones when these cells were stained with Annexin V to detect apoptosis and with 7-aminoactinomycin D to quantify necrosis (Figure 2C). The percentage of dead cells in the right upper and lower quadrants represented 12.5 ± 1.2%, 8.2 ± 1.2% and 9.5 ± 2.1% ($N = 3$, ns) for Hela EV, HeLa Cx37-319S and HeLa Cx37-319P, respectively.

Predicted phosphorylation site for GSK-3 on Cx37-319S and Cx37-319P

Cx37 is a phosphoprotein and may display a shift in electrophoretic mobility on reducing SDS–polyacrylamide gel electrophoresis due to phosphorylation on serine residues (34). NetPhos analysis of amino acid sequence of Cx37CT (amino acids 233–333) revealed 10 serine phosphorylation consensus sequences in Cx37-319S and 9 in Cx37-319P. Differences involved the region around amino acids 319–321 with the serine at position 319 in Cx37-319S being a putative GSK-3 phosphorylation site. Interestingly, another site for phosphorylation by GSK-3 was found at amino acid 321 in Cx37-319P only (Table I). GSK-3 is a Ser/Thr kinase implicated in multiple cellular processes,

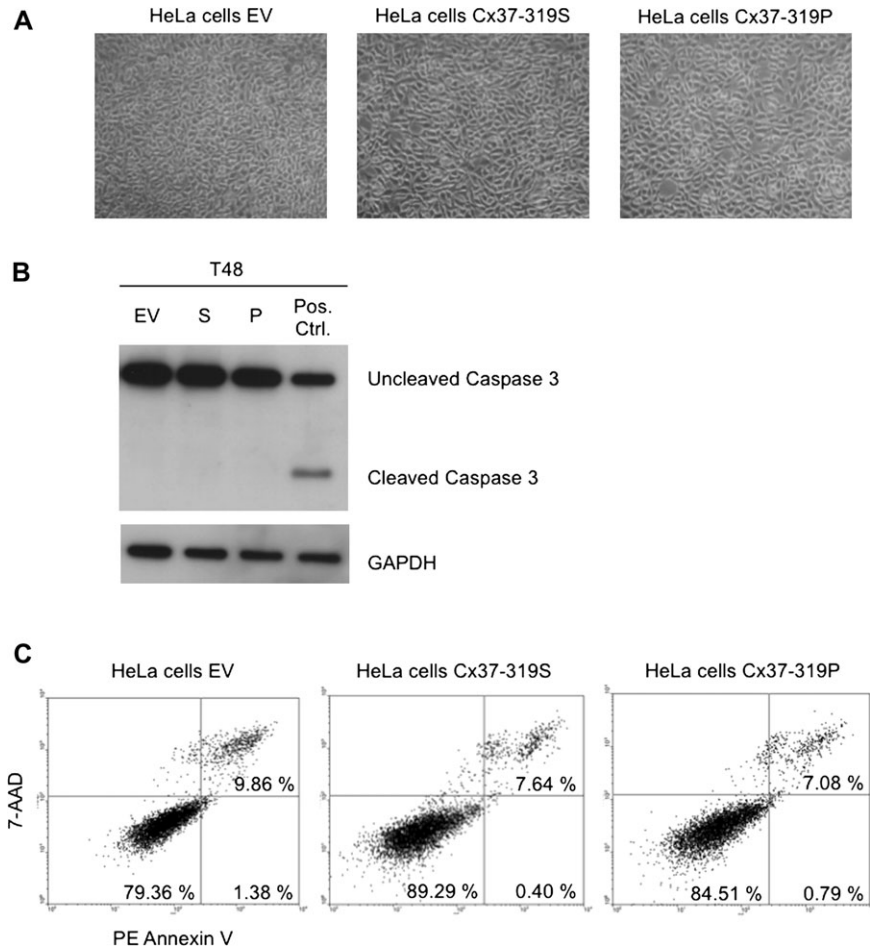

Fig. 2. Cell death in HeLa transfectants. (**A**) Representative photographs of HeLa cells transfected with EV, Cx37-319S and Cx37-319P after 48 h in culture. All cultures have grown to confluence. (**B**) Representative western blot for uncleaved and cleaved Caspase-3 in HeLa transfectants. Positive control (Pos. Ctrl.) was obtained by exposing HeLa cells to 1 μM staurosporine during 24 h. Glyceraldehyde 3-phosphate dehydrogenase (GAPDH) is used as loading control. (**C**) Representative Fluorescence Activated Cell Sorting measurements for Annexin V and 7-aminoactinomycin D (7-AAD). The lower left quadrant shows cells negative for the two staining (viable cells), the lower right quadrant shows cells positive for AnnexinV staining only, representing early apoptosis, and the upper right quadrant shows cells positive for both Annexin V and 7-AAD representing the dead cell fraction.

Table I. Predicted phosphorylation sites on the CT of Cx37-319S and Cx37-319P and predicted kinases associated

Cx37CT-319S				Cx37CT-319P			
a.a. position	Predicted a.a.	Predicted kinases	Score	a.a. position	Predicted a.a.	Predicted kinases	Score
254	T	—		254	T	—	
256	S	—		256	S	—	
275	**S**	**GSK-3**	**0**	**275**	**S**	**GSK-3**	**0.53**
		cdc2	0.58			cdc2	0.58
		cdk5	0.66			cdk5	0.66
		P38MAPK	0.56			P38MAPK	0.56
285	S	CKII	0.56	285	S	CKII	0.56
286	S	—		286	S	—	
295	T	CKII	0.54	295	T	CKII	0.54
		cdc2	0.50			cdc2	0.50
302	S	PKC	0.54	302	S	PKC	0.54
319	**S**	**GSK-3**	**0.51**	319	—	—	
		cdk5	0.62				
321	S	cdc2	0.56	**321**	**S**	**GSK-3**	**0.52**
						cdc2	0.53
324	S	PKC	0.72	324	S	PKC	0.63
325	S	PKC	0.71	325	S	PKC	0.71
						RSK	0.50
328	S	PKC	0.86	328	S	PKC	0.86

a.a., amino acid; S, serine; T, threonine; cdc2, cell division cycle 2; cdk5, cyclin-dependent kinase 5; MAPK, mitogen-activated protein kinase; CKII, casein kinase II; PKC, protein kinase C; RSK, ribosomal S6 kinase. Analyses were performed with the NetPhos 2.0 Server and with the NetPhosK 1.0 server. Consensus sites for GSK-3 are shown in bold.

including cell proliferation (reviewed in refs. 27,28). An additional site for GSK-3 phosphorylation may be found at amino acid 275 in both Cx37CTs (Table 1). Importantly, action of GSK-3 on a substrate in living cells requires a priming phosphate at $n + 4$ (where n is the site of phosphorylation for GSK-3) (35,36). This implies that phosphorylation on position 275, 319 or 321 by GSK-3 will need a priming phosphate, respectively, on position 279, 323 or 325. Detailed analysis of the amino acid sequence of Cx37CT does not show phosphorylation sites on position 279 or 323 but predicts a serine on position 325 that may be phosphorylated by protein kinase C or ribosomal S6 kinase. Because this priming phosphorylation site is only present in Cx37CT-319P, one would expect that only this polymorphic isoform may be phosphorylated by GSK-3 in living cells.

Phosphorylation of Cx37CT by GSK-3β

GSK-3 appears constitutively active in most cells, including HeLa cells, and becomes inhibited in response to a variety of agonists as a result of phosphorylation of a single serine residue (Ser9 for GSK-3β and Ser21 for GSK-3α) (37). Several inhibitors of GSK-3 have been identified, including lithium ions and SB415286 (37,38). Lithium acts directly by competing with magnesium and also indirectly by increasing the inhibitory phosphorylation of Ser9 or Ser21 in GSK-3. SB415286 is a specific inhibitor of GSK-3 that acts by competing with ATP, which prevents phosphorylation of substrate (39). To study the effects of GSK-3 on Cx37 phosphorylation, we first determined the optimal condition for limiting GSK-3 activity in HeLa cells. For this purpose, we exposed HeLa cells transfected with Cx37-319S, Cx37-319P or EV to increasing concentrations of the GSK-3 inhibitors LiCl (0, 5, 10, 20 and 40 mM) or SB415286 (0, 5, 10, 25, 50, 75 and 100 μM) during 15 min. As shown in Figure 3A, we observed a significant increase in phospho-GSK-3β and phospho-GSK-3α after exposure to 10 mM LiCl. This effect was similar in all three transfectants (data not shown) and did not further increase with increased concentration of the substance. A significant decrease in phospho-β-catenin, a substrate of GSK-3, was already observed after exposure of HeLa transfectants to 25 μM SB415286 (Figure 3B). Increasing the concentration of SB415286 up to 100 μM revealed a further dose-dependent decrease in phospho-β-catenin. However, doses >50 μM have been shown to exhibit unspecific additional effects (39,40).

As shown in Figure 3C, Cx37CT is phosphorylated by GSK-3β *in vitro*. Under basal conditions (reaction in presence of H_2O or DMSO), the phosphorylation statuses of Cx37CT-319S and Cx37CT-319P are similar. Inhibition of GSK-3β with 10 mM LiCl or 50 μM SB415286 induced a significant reduction in the phosphorylation of Cx37CT-319S and Cx37-319P by GSK-3β ($P < 0.05$). This decrease of phosphorylation was similar between Cx37CT-319S and Cx37-319P when GSK-3β was inhibited by LiCl (53 and 58%, respectively, ns), but enhanced reduction was observed in Cx37CT-319P compared with Cx37CT-319S using the selective SB415286 inhibitor (65 and 51%, respectively; $P < 0.05$). Nevertheless, western blot for Cx37 of HeLa cells treated with 10 mM LiCl during 15 min did not show a shift in electrophoretic mobility (data not shown).

GJIC in Cx37-319S and Cx37-319P transfectants in absence or in presence of GSK-3 inhibitors

Next, we have investigated the subcellular localization of Cx37 in Cx37-319S- and Cx37-319P-expressing HeLa cells by immunofluorescence. As expected for transfected cells, a strong Cx37 immunosignal was observed perinuclearly in both transfectants and incidentally Cx37 immunosignals were detected at the cell-to-cell interface (Figure 4A). The specificity of the immunostaining is illustrated by the total absence of signal in HeLa cells transfected with the EV. The subcellular localization of Cx37 in both Cx37-319S and Cx37-319P transfectants was not affected by treatment with 10 mM LiCl for 15 min (Figure 4A). Both Cx37 polymorphic channels formed functional gap junctions as shown by the extensive cell-to-cell spread of neurobiotin after 3 min of injection (Figure 4B). In contrast, the parental HeLa cells did not show diffusion of neurobiotin to neighboring cells ($N = 7$). Interestingly, the number of cells labelled with neurobiotin was significantly lower in HeLa cells expressing Cx37-319P (3.3 ± 0.8) compared with the ones expressing Cx37-319S (7.7 ± 2.1, $P < 0.05$; Figure 4B and D). The difference in GJIC between Cx37-319S- and Cx37-319P-expressing HeLa cells was not affected by pre-incubation with DMSO, the solvent of SB415286. Interestingly, inhibition of endogenous GSK-3 activity by 10 mM LiCl or 50 μM SB415286 significantly increased GJIC in HeLa cells transfected with Cx37-319P ($P < 0.05$ versus vehicle), whereas it did not affect GJIC in Cx37-319S transfectants (Figure 4D) nor did it affect the absence of coupling in parental HeLa cells ($N = 8$;

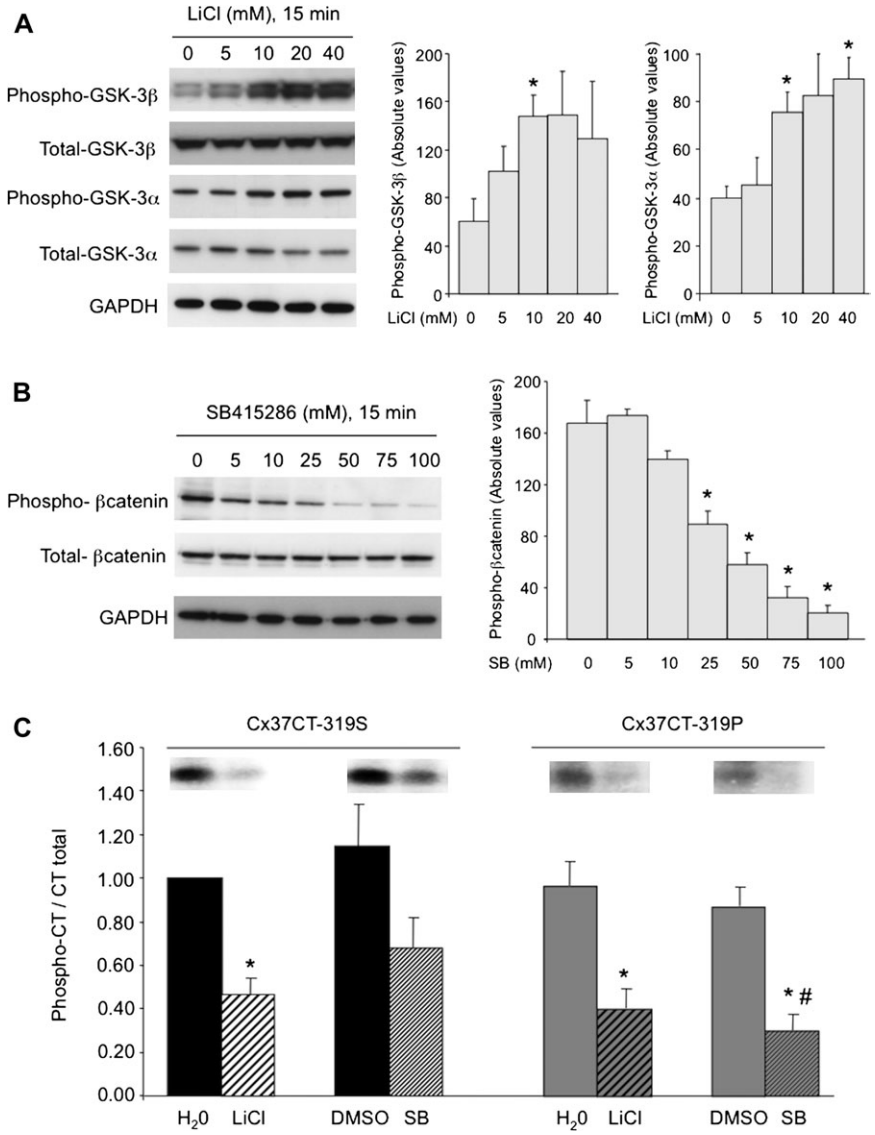

Fig. 3. Phosphorylation of Cx37CT-319S and Cx37-319P by GSK-3β (**A**) Representative western blots for phospho-GSK-3β, total-GSK-3β, phospho-GSK-3α, total-GSK-3α and Glyceraldehyde 3-phosphate dehydrogenase (GAPDH) (loading control) in HeLa cells treated with different concentrations of LiCl during 15 min. As shown by the quantification of western blots, LiCl increased phosphorylation of GSK-3β and GSK-3α in a dose-dependent manner with a maximal effect reached at 10 mM; $N = 3$. Error bars show SEM and $^{*}P < 0.05$ versus control. (**B**) Representative western blots for phospho-β-catenin, total-β-catenin and Glyceraldehyde 3-phosphate dehydrogenase (GAPDH) (loading control) in HeLa cells treated with different concentrations of SB415286 during 15 min. As shown by the quantification of western blots, SB415286 decreased phosphorylation of β-catenin, a target for active GSK-3, in a dose-dependent manner, which reached significance at a dose of 25 μM; $N = 3$. Error bars show SEM and $^{*}P < 0.05$ versus control. (**C**) In basal conditions, GSK-3β phosphorylation of Cx37CT-319S and Cx37CT-319P is similar. Inhibition of GSK-3β activity by 10 mM LiCl limited phosphorylation of both Cx37 isoforms. However, a higher efficacy for Cx37CT-319P was observed with 50 μM SB415286 treatment (SB). Data of six or seven independent experiments were expressed in ratio of phosphorylation status of Cx37CT-319S incubated with H_2O. Error bars show SEM, $^{*}P < 0.05$ versus vehicle and $\#P < 0.05$ versus Cx37CT-319S. Representative radiographs are shown for each condition.

data not shown). To specifically determine the effect of each GSK-3 isoform on GJIC in HeLa cells expressing Cx37-319P or Cx37-319S, we treated these transfectants with siRNA against GSK-3β or GSK-3α or with control siRNA for 48 or 60 h. The optimal concentration of each siRNA and the optimal duration of incubation were determined in a separate experiment (data not shown). As shown in Figure 4C, incubation with 50 nM GSK-3β siRNA for 48 h specifically decreased the expression of GSK-3β without affecting the expression of GSK-3α. Conversely, treatment with 25 nM GSK-3α siRNA for 60 h limited GSK-3α expression without affecting GSK-3β. The efficacy of each siRNA was similar between HeLa Cx37-319S cells and HeLa Cx37-319P cells. We then performed dye injections in HeLa transfectants treated with these different siRNAs. As shown in Figure 4C, decreasing the expression of GSK-3β induced a significant increase of the spread of neurobiotin between Cx37-319P-expressing cells but not between Cx37-319S-expressing cells. In contrast, decreasing the expression of GSK-3α did not modify GJIC in HeLa cells transfected with Cx37-319S or Cx37-319P. Finally, control siRNA was without effect on GJIC in both clones.

The cell-to-cell spread of neurobiotin might be influenced by cell density, we therefore measured electrical coupling between pairs of cells using the dual whole-cell patch clamp approach. We found that both HeLa- and SK-HEP-1-transfected cells with Cx37-319S showed increased g_j as compared with Hela or SK-HEP-1 cells expressing Cx37-319P (Figure 5). Importantly, inhibition of endogenous GSK-3 activity by 10 mM LiCl for 15 min significantly increased g_j in cells transfected with Cx37-319P ($P < 0.05$), whereas it did not affect g_j in Cx37-319S transfectants (Figure 5).

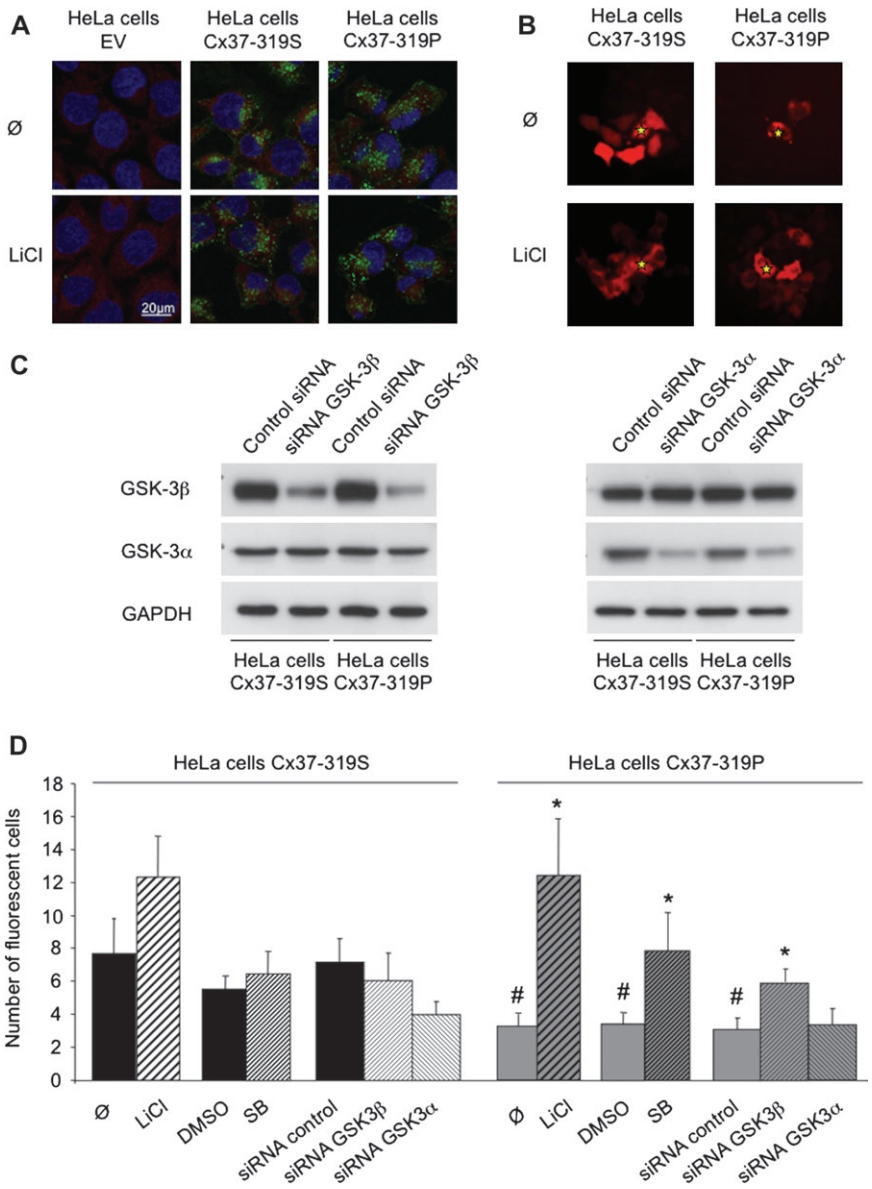

Fig. 4. Cell-to-cell coupling in HeLa cells expressing Cx37-319S or Cx37-319P. (**A**) Immunofluorescent staining of HeLa cells transfected with EV, Cx37-319S or Cx37-319P. Whereas Cx37 was absent in HeLa cells transfected with EV, it was readily detected in HeLa cells transfected with Cx37-319S or Cx37-319P. Cx37 was mainly detected intercellularly in Cx37-319S- or Cx37-319P-expressing cells, and this distribution was not different after LiCl treatment. (**B**) Intercellular communication was measured by microinjection of Lucifer yellow and neurobiotin during 3 min. Images are representative examples of neurobiotin diffusion in HeLa Cx37-319S and Cx37-319P cells submitted or not to treatment with 10 mM LiCl for 15 min before the microinjection. Asterisks indicate the microinjected cells. (**C**) Representative western blots of GSK-3β and GSK-3α in HeLa Cx37-319S and HeLa Cx37-319P cells treated with control siRNA, siRNA for GSK-3β or GSK-3α. GSK-3β siRNA induced a specific decrease of expression of GSK-3β without affecting GSK-3α expression, and GSK-3α siRNA blocked specifically GSK-3α expression without affecting GSK-3β expression. There was no difference of siRNA efficacy between HeLa Cx37-319S and Cx37-319P cells. (**D**) Intercellular communication was measured by microinjection of Lucifer yellow and neurobiotin during 3 min. Inhibition of GSK-3 was induced by adding 10 mM LiCl or 50 µM SB415286 15 min before the microinjections. Alternatively, cells were transfected with siRNA specifically inhibiting GSK-3α or GSK-3β. In basal conditions, GJIC between Cx37-319P-transfected cells was significantly lower compared with GJIC between Cx37-319S transfectants. Inhibition of GSK-3 by LiCl or SB415286 (SB) 15 min before the microinjections significantly increased GJIC between Cx37-319P transfectants, whereas GJIC between Cx37-319S-transfected cells remained unchanged. Specific decrease of GSK-3β expression with siRNA significantly increased GJIC in HeLa Cx37-319P cells but not in HeLa Cx37-319S cells. Control siRNA and siRNA for GSK-3α did not modify GJIC in the two clones. Results are presented as mean of 6–13 microinjections for each condition. Error bars show SEM and $^{*}P < 0.05$ versus vehicle and $\#P < 0.05$ versus HeLa Cx37-319S cells.

Discussion

GJIC has previously been shown to regulate cellular proliferation and has been implicated in cancer. In a small epidemiological study, a polymorphism in the human Cx37 gene (*C1019T*) has been suggested to be associated with susceptibility to angiosarcomas (24). In the present study, we have compared cell proliferation between communication-deficient cells (HeLa and SK-HEP-1 cells) stably expressing similar levels of Cx37-319S and Cx37-319P. Our results show decreased proliferation of HeLa and SK-HEP-1 cells expressing Cx37-319P. NetPhos analysis of the CT tail of Cx37 revealed GSK-3 phosphorylation sites in the region around amino acid 319. *In vitro* kinase assays, in presence of active recombinant GSK-3β and Cx37CT-319S or Cx37CT-319P, demonstrated that this GSK-3 was effectively capable to phosphorylate Cx37CT. We observed reduced GJIC between Cx37-319P-transfected tumour cells compared with

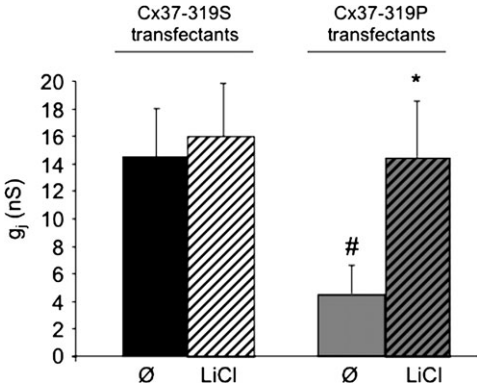

Fig. 5. Gap junctional conductance in cells expressing Cx37-319S or Cx37-319P. Gap junctional conductance (g_j) was measured by dual whole-cell patch clamp on HeLa or SK-HEP-1 cells pairs stably expressing similar amount of Cx37-319P or Cx37-319S. Inhibition of GSK-3 was induced by adding 10 mM LiCl 15 min before the recordings. In basal conditions, g_j between Cx37-319P-transfected cells was significantly lower compared with g_j between Cx37-319S transfectants. Inhibition of GSK-3 by LiCl significantly increased g_j between Cx37-319P transfectants whereas g_j between Cx37-319S-transfected cells remained unchanged. Because HeLa and SK-HEP-1 transfectants showed similar behaviour, g_j values were pooled for graphic presentation. Under control conditions, $N = 4$ for HeLa Cx37-319P and $N = 4$ for SK-HEP-1-Cx37-319P and $N = 3$ for HeLa Cx37-319S and $N = 4$ for SK-HEP-1-Cx37-319S. In the presence of LiCl, $N = 7$ for HeLa Cx37-319P and $N = 4$ SK-HEP-1-Cx37-319P and $N = 4$ for HeLa Cx37-319S and $N = 2$ for SK-HEP-1-Cx37-319S.

cells transfected with Cx37-319S. Finally, specific inhibition of GSK-3β equilibrated cell-to-cell communication in Cx37-319S- and Cx37-319P-expressing HeLa cells. Overall, our data indicate functional effects of the Cx37 C1019T polymorphism on GJIC that might contribute to tumour cell growth.

Communication-deficient HeLa cells are commonly used to study the effects of specific connexins (f.e. Cx43, Cx40, Cx32 or Cx26) on cellular proliferation (6). Interestingly, expression of Cx43 and Cx26 appeared to decrease cell proliferation, whereas expression of Cx32 and Cx40 was without effect. Recently, Burt *et al.* (41) have shown that expression of mouse Cx37 slowed cell cycle progression in communication-deficient rat insulinoma cells. In our models of HeLa and SK-HEP-1 cells expressing equal amounts of Cx37, Cx37-319S failed to modify cellular proliferation and Cx37-319P limited it. Thus, the suppressive action of Cx37 on cell proliferation seems to be specific for the polymorphic isoform studied.

Because Cx37 is mostly expressed in endothelial cells, its role in tumour development was first studied in endothelial-derived tumours such as angiosarcomas. Although Cx37 mutations have been detected in hepatic angiosarcomas from rats treated with vinyl chloride, they are probably not crucial for tumour development as they are only rare events (19). Interestingly, these authors detected Cx37 in endothelial cells of normal liver, but none of the angiosarcomas showed Cx37 immunoreactivity, suggestive for disturbed Cx37-mediated GJIC in these tumours. In human, two Cx37 gene polymorphisms have been studied in relation to cancer. A single-nucleotide polymorphism leading to an amino acid change (valine-to-isoleucine) at codon 130 in the cytoplasmic loop of the Cx37 protein showed a similar distribution in breast and lung cancer patients versus healthy donors (42). However, genotyping for a second single-nucleotide polymorphism leading to an amino acid change (proline-to-serine) at codon 319 in the cytoplasmic tail of Cx37 revealed the possibility that the Cx37-319S allele might predispose to vinyl chloride-associated angiosarcoma in human (24). In agreement with this study, we show that expression of Cx37-319P limited the proliferation of both HeLa and SK-HEP-1 cells, tumour cells of epithelial and endothelial origin, whereas the expression of Cx37-319S was without effect. While the number of samples in the afore-mentioned epidemiological study (24) was too small to allow for firm conclusions, it should be noted that most phosphorylation sequences reside in Cx37CT and that, in analogy to other connexins (43), changes in phosphorylation state might affect the function of Cx37, including cell-to-cell communication.

Implications of connexins in tumourigenesis depend on their localization, their quantity and their phosphorylation status. Various studies suggest a possible link between kinase activation, connexin phosphorylation and cell cycle progression (44,45). Importantly, Larson *et al.* (34) have demonstrated that Cx37 may be phosphorylated on serine, tyrosine or threonine residues; they did not, however, identify the kinases implicated in this process. In this study, we performed detailed NetPhos analysis on Cx37CT and found that the region around the polymorphic position 319 may be a site for phosphorylation by GSK-3. GSK-3 is a ubiquitous Ser/Thr kinase that was first described for its role in the phosphorylation and inactivation of glycogen synthase (46). In mammals, two isoforms of GSK-3 have been described: GSK-3α and GSK-3β. GSK-3β has been extensively studied and appeared to be implicated in cellular proliferation and cancer (reviewed in refs. 27,28). In fact, GSK-3β might act both as a 'tumour suppressor' or as a 'tumour promoter' depending on the organ studied (47). Unlike most protein kinases, GSK-3β is constitutively active in resting cells and >40 proteins have been shown to be a substrate for GSK-3β. Here, we identify Cx37 as a new substrate for GSK-3β. Using an *in vitro* kinase assay, we demonstrate that Cx37CT-319S and Cx37CT-319P are subject to phosphorylation by GSK-3β. It has been described that a priming phosphorylation at $n + 4$ increases the efficacy of GSK-3 substrate phosphorylation by 100- to 1000-fold in living cells (36,48). Sequence analysis of the polymorphic Cx37 isoforms showed that only Cx37-319P has a protein kinase C phosphorylation site at $n + 4$ (serine on position 325), suggesting preferential phosphorylation of this isoform by GSK-3. On position 275, it seems that a phosphorylation site for GSK-3 could exist, but the priming phosphorylation site is not present at the position 279 suggesting a low efficacy of GSK-3 on this site. Although our *in vitro* kinase assays revealed the possibility of GSK-3-dependent phosphorylation for both Cx37-319P and Cx37-319S when substrate and kinase were present in excess, inhibition of GSK-3β by the specific inhibitor SB415286 had a larger effect on phosphorylation efficacy on Cx37CT-319P than on Cx37CT-319S. Unfortunately, it is not possible to measure the phosphorylation of Cx37 by GSK-3 directly in cells due to the presence of multiple other kinases predicted to phosphorylate Cx37 (Table 1). Therefore, we assume that in living cells with physiological quantities of Cx37 and GSK-3, GSK-3 will preferentially phosphorylate Cx37-319P.

GSK-3 is an endogenously active kinase in HeLa cells, thus we expect that Cx37-319P is phosphorylated in our cells under basal conditions. We observed low cell-to-cell communication, as measured by neurobiotin diffusion, in HeLa Cx37-319P transfectants compared with HeLa cells expressing equal amounts of Cx37-319S. Following inhibition of GSK-3 with LiCl or SB415286, phosphorylation of Cx37CT-319P decreased and GJIC in HeLa Cx37-319P transfectants increased. Using isoform specific siRNAs, we showed that limitation of GSK-3β expression, but not of GSK-3α expression, induced an increase in GJIC between HeLa Cx37-319P cells. Differences in substrate specificity between the two isoforms of GSK-3 have been described before (see ref. for review 47). In general, phosphorylation of GSK-3 substrates leads to their inactivation (47). Our results are in accordance with these observations; the phosphorylation of Cx37-319P by GSK-3 is associated with low Cx37-319P channel function. In contrast, Cx37-319S channels showed a higher basal GJIC and their function seemed not affected by GSK-3 inhibitors. It is therefore likely that, contrary to *in vitro* kinase assay, GSK-3 does not phosphorylate Cx37-319S under physiological conditions or, alternatively, phosphorylation of Cx37-319S does not affect its gap junction channel function. In this respect, mutation of the priming Ser325 site in Cx37-319P might help to obtain further insight in post-translational modifications of Cx37CT in link to its function. Finally, it has been recently demonstrated that 24 h treatment of skeletal myoblasts with LiCl modified Cx43 expression and gap junctional communication

(49,50). This long-term regulation of Cx43 expression by LiCl seemed to involve the Wnt signaling pathway, affecting both the transcription and phosphorylation of the protein. Together with our data, these studies show that GSK-3 is important for the regulation of connexins at multiple levels, varying from transcription and expression to channel function.

The first observations linking gap junction function and cell growth control have been described ∼40 years ago. Since then, a tremendous amount of evidence has shown that connexins are somehow linked to cell proliferation and cancer, but the mechanism is far from being resolved (see ref. for review 7). More recent studies have demonstrated that Cx43-mediated GJIC may modify gene expression of cancer cells by selectively permitting the passage of some intracellular metabolites (51,52). In our study, only the expression of Cx37-319P limited proliferation in HeLa cells and SK-HEP-1 cells. The differences in anti-proliferative properties between Cx37-319S and Cx37-319P might be due to different channel selectivity for gene expression-regulating metabolites between these cells.

In conclusion, our results suggest that GSK-3β by maintaining Cx37-319P endogenously in a phosphorylated state limits GJIC and reduces proliferation of multiple types of tumour cells. These results support the tumour suppressor role of GSK-3β and Cx37. Moreover, they underline the importance for large epidemiological studies towards a possible association between the Cx37 C1019T polymorphism and the development of endothelial-derived tumours.

Funding

Swiss National Science Foundation (PPOOA-116897 and 310030-127551 to B.R.K., 310000-119739 to M.C.); a joint grant from the Swiss National Science Foundation, the Swiss Academy of Medical Sciences and the Velux Foundation (323630-123735 to A.P.); Fondation Novartis to B.R.K.; Fondation Dr H.Dubois-Ferrièrre Dinu Lipatti to B.R.K.

Acknowledgements

The authors thank Sophie Crespin, Robert Weingart, Jean-Paul Derouette and Hamdy Shamban for helpful discussion.

Conflict of Interest Statement: None declared.

References

1. Goodenough,D.A. *et al*. (2003) Beyond the gap: functions of unpaired connexon channels. *Nat. Rev. Mol. Cell Biol.*, **4**, 285–294.
2. Saez,J.C. *et al*. (2003) Plasma membrane channels formed by connexins: their regulation and functions. *Physiol. Rev.*, **83**, 1359–1400.
3. Brisset,A.C. *et al*. (2009) Connexins in vascular physiology and pathology. *Antioxid. Redox Signal.*, **11**, 267–282.
4. White,T.W. (2003) Nonredundant gap junction functions. *News Physiol. Sci.*, **18**, 95–99.
5. Thomas,M.A. *et al*. (2002) Interaction of connexins with protein partners in the control of channel turnover and gating. *Biol. Cell*, **94**, 445–456.
6. Mesnil,M. *et al*. (1995) Negative growth control of HeLa cells by connexin genes: connexin species specificity. *Cancer Res.*, **55**, 629–639.
7. Cronier,L. *et al*. (2009) Gap junctions and cancer: new functions for an old story. *Antioxid. Redox Signal.*, **11**, 323–338.
8. Defamie,N. *et al*. (2001) Disruption of gap junctional intercellular communication by lindane is associated with aberrant localization of connexin43 and zonula occludens-1 in 42GPA9 Sertoli cells. *Carcinogenesis*, **22**, 1537–1542.
9. Govindarajan,R. *et al*. (2002) Impaired trafficking of connexins in androgen-independent human prostate cancer cell lines and its mitigation by alpha-catenin. *J. Biol. Chem.*, **277**, 50087–50097.
10. de Feijter,A.W. *et al*. (1996) Localization and function of the connexin 43 gap-junction protein in normal and various oncogene-expressing rat liver epithelial cells. *Mol. Carcinog.*, **16**, 203–212.
11. Eghbali,B. *et al*. (1991) Involvement of gap junctions in tumorigenesis: transfection of tumor cells with connexin 32 cDNA retards growth *in vivo*. *Proc. Natl Acad. Sci. USA*, **88**, 10701–10705.
12. Mehta,P.P. *et al*. (1991) Incorporation of the gene for a cell-cell channel protein into transformed cells leads to normalization of growth. *J. Membr. Biol.*, **124**, 207–225.
13. Zhu,D. *et al*. (1991) Transfection of C6 glioma cells with connexin 43 cDNA: analysis of expression, intercellular coupling, and cell proliferation. *Proc. Natl Acad. Sci. USA*, **88**, 1883–1887.
14. Naus,C.C. *et al*. (1992) *In vivo* growth of C6 glioma cells transfected with connexin43 cDNA. *Cancer Res.*, **52**, 4208–4213.
15. Rose,B. *et al*. (1993) Gap-junction protein gene suppresses tumorigenicity. *Carcinogenesis*, **14**, 1073–1075.
16. Mesnil,M. *et al*. (2005) Defective gap junctional intercellular communication in the carcinogenic process. *Biochim. Biophys. Acta*, **1719**, 125–145.
17. Mandelboim,O. *et al*. (1994) CTL induction by a tumour-associated antigen octapeptide derived from a murine lung carcinoma. *Nature*, **369**, 67–71.
18. Berke,G. *et al*. (2003) Connexin 37 gene is not mutated in lung carcinomas 3LL and CMT. *Cancer Lett.*, **195**, 67–72.
19. Saito,T. *et al*. (1997) Connexin 37 mutations in rat hepatic angiosarcomas induced by vinyl chloride. *Cancer Res.*, **57**, 375–377.
20. Chanson,M. *et al*. (2007) Connexin37: a potential modifier gene of inflammatory disease. *J. Mol. Med.*, **85**, 787–795.
21. Morel,S. *et al*. (2009) Connexins participate in the initiation and progression of atherosclerosis. *Semin. Immunopathol.*, **31**, 49–61.
22. Wong,C.W. *et al*. (2006) Connexin37 protects against atherosclerosis by regulating monocyte adhesion. *Nat. Med.*, **12**, 950–954.
23. Derouette,J.P. *et al*. (2009) Functional differences between human Cx37 polymorphic hemichannels. *J. Mol. Cell. Cardiol.*, **46**, 499–507.
24. Saito,T. *et al*. (2000) Human hemangiosarcomas have a common polymorphism but no mutations in the connexin37 gene. *Int. J. Cancer*, **86**, 67–70.
25. Jennings,R.C. *et al*. (1978) Haemangioendothelioma (Kupffer cell angiosarcoma), myelofibrosis, splenic atrophy, and myeloma paraproteinaemia after parenteral thorotrast administration. *J. Clin. Pathol.*, **31**, 1125–1132.
26. Pirastu,R. *et al*. (1990) Mortality from liver disease among Italian vinyl chloride monomer/polyvinyl chloride manufacturers. *Am. J. Ind. Med.*, **17**, 155–161.
27. Eldar-Finkelman,H. (2002) Glycogen synthase kinase 3: an emerging therapeutic target. *Trends Mol. Med.*, **8**, 126–132.
28. Jope,R.S. *et al*. (2007) Glycogen synthase kinase-3 (GSK3): inflammation, diseases, and therapeutics. *Neurochem. Res.*, **32**, 577–595.
29. Wilkins,J.A. *et al*. (1991) Beta 1 integrin-mediated lymphocyte adherence to extracellular matrix is enhanced by phorbol ester treatment. *Eur. J. Immunol.*, **21**, 517–522.
30. Blom,N. *et al*. (2004) Prediction of post-translational glycosylation and phosphorylation of proteins from the amino acid sequence. *Proteomics*, **4**, 1633–1649.
31. Duffy,H.S. *et al*. (2002) pH-dependent intramolecular binding and structure involving Cx43 cytoplasmic domains. *J. Biol. Chem.*, **277**, 36706–36714.
32. Pfenniger,A. *et al*. (2010) The gap junction protein Cx37 interacts with eNOS in endothelial cells. *Arterioscler. Thromb. Vasc. Biol.*, **30**, 827–834.
33. Chanson,M. *et al*. (1999) Defective regulation of gap junctional coupling in cystic fibrosis pancreatic duct cells. *J. Clin. Invest.*, **103**, 1677–1684.
34. Larson,D.M. *et al*. (2000) Functional expression and biochemical characterization of an epitope-tagged connexin37. *Mol. Cell Biol. Res. Commun.*, **3**, 115–121.
35. Fiol,C.J. *et al*. (1987) Formation of protein kinase recognition sites by covalent modification of the substrate. Molecular mechanism for the synergistic action of casein kinase II and glycogen synthase kinase 3. *J. Biol. Chem.*, **262**, 14042–14048.
36. Doble,B.W. *et al*. (2003) GSK-3: tricks of the trade for a multi-tasking kinase. *J. Cell Sci.*, **116**, 1175–1186.
37. Cohen,P. *et al*. (2004) GSK3 inhibitors: development and therapeutic potential. *Nat. Rev. Drug Discov.*, **3**, 479–487.
38. Frame,S. *et al*. (2001) GSK3 takes centre stage more than 20 years after its discovery. *Biochem. J.*, **359**, 1–16.
39. Meijer,L. *et al*. (2004) Pharmacological inhibitors of glycogen synthase kinase 3. *Trends Pharmacol. Sci.*, **25**, 471–480.
40. Coghlan,M.P. *et al*. (2000) Selective small molecule inhibitors of glycogen synthase kinase-3 modulate glycogen metabolism and gene transcription. *Chem. Biol.*, **7**, 793–803.
41. Burt,J.M. *et al*. (2008) Connexin 37 profoundly slows cell cycle progression in rat insulinoma cells. *Am. J. Physiol. Cell Physiol.*, **295**, C1103–C12.
42. Krutovskikh,V. *et al*. (1996) Human connexin 37 is polymorphic but not mutated in tumours. *Carcinogenesis*, **17**, 1761–1763.

43. Takens-Kwak,B.R. *et al*. (1992) Cardiac gap junctions: three distinct single channel conductances and their modulation by phosphorylating treatments. *Pflugers Arch.*, **422**, 198–200.
44. Dang,X. *et al*. (2003) The carboxy-tail of connexin-43 localizes to the nucleus and inhibits cell growth. *Mol. Cell. Biochem.*, **242**, 35–38.
45. Doble,B.W. *et al*. (2004) Phosphorylation of serine 262 in the gap junction protein connexin-43 regulates DNA synthesis in cell-cell contact forming cardiomyocytes. *J. Cell Sci.*, **117**, 507–514.
46. Embi,N. *et al*. (1980) Glycogen synthase kinase-3 from rabbit skeletal muscle. Separation from cyclic-AMP-dependent protein kinase and phosphorylase kinase. *Eur. J. Biochem.*, **107**, 519–527.
47. Rayasam,G.V. *et al*. (2009) Glycogen synthase kinase 3: more than a namesake. *Br. J. Pharmacol.*, **156**, 885–898.
48. Thomas,G.M. *et al*. (1999) A GSK3-binding peptide from FRAT1 selectively inhibits the GSK3-catalysed phosphorylation of axin and beta-catenin. *FEBS Lett.*, **458**, 247–251.
49. Du,W.J. *et al*. (2008) Lithium chloride regulates connexin43 in skeletal myoblasts *in vitro*: possible involvement in Wnt/beta-catenin signaling. *Cell Commun. Adhes.*, **15**, 261–271.
50. Du,W.J. *et al*. (2009) Lithium chloride preconditioning optimizes skeletal myoblast functions for cellular cardiomyoplasty *in vitro* via glycogen synthase kinase-3beta/beta-catenin signaling. *Cells Tissues Organs*, **190**, 11–19.
51. Goldberg,G.S. *et al*. (2002) Gap junctions between cells expressing connexin 43 or 32 show inverse permselectivity to adenosine and ATP. *J. Biol. Chem.*, **277**, 36725–36730.
52. Upham,B.L. *et al*. (2003) Reduced gap junctional intercellular communication and altered biological effects in mouse osteoblast and rat liver oval cell lines transfected with dominant-negative connexin 43. *Mol. Carcinog.*, **37**, 192–201.

Received January 15, 2010; revised June 29, 2010; accepted July 27, 2010